Trapped modes due to narrow cracks in thin simply-supported elastic plates

R. Porter*, D.V. Evans

School of Mathematics, University of Bristol, Bristol, BS8 1TW, UK.

Abstract

We consider an elastic plate of infinite length and constant width supported simply along its two parallel edges and having a finite length crack along its centreline. In particular, we look for and find trapped modes (localised oscillations) in the presence of the crack. An explicit wide-spacing approximation based on the Wiener-Hopf technique applied to incident wave scattering by semi-infinite cracks is complemented by an exact formulation of the problem in the form of integro-differential equations. An application of a Galerkin method for the numerical calculation of results from the latter method leads to a novel explicit 'small-spacing' approximation. In combination with the wide-spacing results this is shown to provide accurate results for all lengths of crack.

Keywords: trapped modes, thin elastic plates, thin cracks, Wiener-Hopf method, integro-differential equations

1. Introduction

In a recent paper, Porter [14] provided numerical evidence for localised time-harmonic out-of-plane oscillations in a thin elastic plate of infinite extent but constant width and simply supported along its two parallel edges. The mechanism by which these undamped bending waves remain trapped is provided by the presence of a circular hole cut out of the centreline of the strip. Crucially, use is made of the fact that, below a certain non-zero critical frequency, free waves are prohibited from propagating along the strip

*Corresponding author

Email address: richard.porter@bris.ac.uk (R. Porter)

to infinity. Thus it was shown in Porter [14] that trapped modes with displacements both symmetric and antisymmetric about the centreline of the strip are possible when the edge of the circular hole is free and for any radius provided that the circular hole is contained within the strip. In constrast no such modes are found when the edge of the circular hole is clamped.

The motivation behind the idea of Porter [14] came from earlier studies into the trapping of acoustic waves by sound-hard circles in parallel-walled acoustic waveguides (Callan et al. [2]) in which similar critical frequencies could be generated by considering motions with particular symmetries. Indeed, the method employed by Porter [14] of using multipole expansions followed methods pioneered in the work of Callan et al. [2].

A large body of work on the subject of trapped waves in acoustics (whose formulation also applies to other physical settings such as surface waves on water, quantum wires, electromagnetics etc) in parallel-walled waveguide domains emerged around the same time as the work of Callan et al. [2]; see Linton & McIver [9] for a comprehensive review. This included the work of Evans [5] who gave a constructive proof of trapped modes for a waveguide containing a sufficiently-long rigid plate along the centreline. Earlier, Evans & Linton [4] had used numerical methods in considering rectangular obstacles in waveguides with the thin plate being a limiting case. Thus it was demonstrated that trapped waves exist for a variety of obstacles in waveguides and, in 1994, Evans et al. [3] proved the existence of trapped waves for any symmetric sound-hard obstacle placed in an acoustically-hard walled waveguide, including the geometry considered by Evans [5].

Given this background, it would be very surprising if circular holes with free edges, as considered by Porter [14], were the only geometrical configuration capable of supporting trapped modes in thin elastic plate waveguides. Thus here we consider a geometric configuration in common with that considered by Evans [5], whereby a finite length cut – or crack – is placed along the centreline of the waveguide. Our primary aim is to provide strong evidence for the existence of trapped modes for such a configuration. A secondary purpose is to demonstrate analytical methods for doing this effectively.

Methods for solving problems involving thin cracks in elastic plates in a variety of settings have been considered by numerous authors. For example, Norris & Wang [11] sought the solution to incident plane wave scattering by a semi-infinite straight-line crack in an unbounded elastic plate using the Wiener-Hopf technique. Around the same time, Andronov & Belinskii [1] used Fourier transform methods to develop integro-differential equations

for wave scattering by straight cuts of finite length, again spatially in unbounded plates. This was later extended to multiple finite length cracks in a slightly more complicated model involving elastic plates bounded below by an incompressible fluid of finite depth (a model for cracks in ice sheets) by Porter & Evans [16]. Like Andronov & Belinskii [1], they used a Fourier transform approach to develop integro-differential equations. They also used an expansion of the unknowns in those equations suggested by Andronov & Belinskii [1] to reduce the problem to the solution of a rapidly convergent infinite system of equations.

The approach taken in this paper is two-fold. First we develop a so-called wide-spacing approximation in which the canonical problem of the scattering of waves incident from infinity along a waveguide containing a crack of semi-infinite extent is considered. It is shown in Section 3 using the Wiener-Hopf technique, similar to that described briefly in Evans & Linton [4], that, for frequencies below the critical first cut-off frequency of the waveguide, waves are totally reflected and simple explicit expressions are given for the phase of the complex reflected wave amplitude. This is used to provide estimates of trapped mode configurations on the assumption that the crack is sufficiently long. A second approach, outlined in Section 4 is, in common with the Wiener-Hopf method, based on Fourier transforms and results in integro-differential equations. These are converted to infinite systems of algebraic equations using the same Galerkin approach used in Porter & Evans [16]. This motivates a novel explicit 'small-spacing' approximation to complement the wide-spacing approximation of the earlier section based upon a one-term truncation of the infinite system of equations. In Section 5 it is shown how both types of approximation compare with accurate results from a converged truncation of the system of equations based on the integral equation formulation. It is demonstrated that both approximations work well beyond the assumed limits of applicability.

Finally in Section 6 we summarise the work and discuss features of the solution method, such as not requiring knowledge of the roots of dispersion equations, that make the approaches used here attractive and adaptable to other problems.

2. Formulation of the problem

We consider an infinitely-long rectangular strip, $-1 < y < 1$, $-\infty < x < \infty$ occupied by a thin elastic plate of thickness h whose time-harmonic

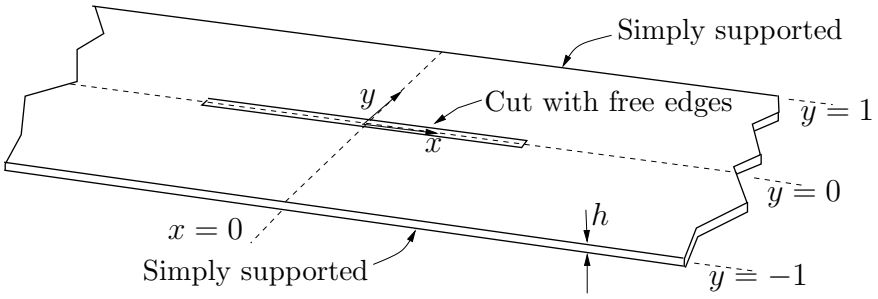

Figure 1: Geometry of the problem.

vibrations described by the function $\Re\{u(x,y)\mathrm{e}^{-\mathrm{i}\omega t}\}$ are perpendicular to the plane it occupies in equilibrium. In the strip

$$(\Delta^2 - k^4)u = 0 \tag{1}$$

is satisfied by $u(x,y)$ where $\Delta = \partial_{xx} + \partial_{yy}$ and $k = \rho h\omega^2/D$ in terms of ρ, the areal density of the plate and D, the flexural rigidity defined as $\frac{1}{12}Eh^3/(1-\nu)$ in terms of the Youngs modulus E and the Poission ratio ν. All lengths are scaled by the fixed width 2 of the plate.

On the lateral boundaries of the strip the elastic plate is simply (roller) supported, so that

$$u = 0, \quad \text{and} \quad u_{yy} = 0, \qquad \text{on } |y| = 1,\ -\infty < x < \infty. \tag{2}$$

Along the centreline, the plate is cut on $x \in \mathcal{C}$, where $\mathcal{C} = \{x : |x| < a\}$ so that here

$$\left.\begin{aligned} (\mathcal{B}u)(x) \equiv u_{yy}(x,0) + \nu u_{xx}(x,0) = 0, \\ (\mathcal{S}u)(x) \equiv u_{yyy}(x,0) + (2-\nu)u_{xxy}(x,0) = 0, \end{aligned}\right\} \qquad x \in \mathcal{C} \tag{3}$$

representing the vanishing of bending moment and shear stress on the free edges.

The geometric symmetry about $y = 0$ allows us to consider solutions of (1)–(3) which are symmetric/antisymmetric about $y = 0$. We denote such solutions by $u^{s/a}(x,y)$ such that

$$u^s(x,y) = u^s(x,-y) \tag{4}$$

and

$$u^a(x,y) = -u^a(x,-y). \tag{5}$$

It follows that, along the centreline away from the cut,

$$\left.\begin{aligned} u^a(x,0) &= 0, \\ u^s_y(x,0) &= 0, \end{aligned}\right\} \qquad x \notin \mathcal{C}. \tag{6}$$

We remark that since u and its derivatives are continuous in the plate and away from the cut, it follows that both $(\mathcal{B}u^a)(x) = 0$ for and $(\mathcal{S}u^s)(x) = 0$ for $x \notin \mathcal{C}$ and hence

$$(\mathcal{B}u^a)(x) = 0, \qquad (\mathcal{S}u^s)(x) = 0, \qquad \text{for all } x. \tag{7}$$

So-called Meixner conditions must also be imposed, ensuring that the energy assoicated with the geoemetric singularity at either end-point of the crack is bounded. Here, we must insist that

$$\lim_{r\to 0}\left\{r^{-3/2}u(x,y)\right\} \to C_1, \qquad \lim_{r\to 0}\left\{r^{-1/2}u_r(x,y)\right\} \to C_2, \tag{8}$$

where C_1, C_2 are constants and r measures the radial distance from the edge of the crack to a point on the plate.

In seeking trapped modes, we insist that wave energy is prohibited from propagating along the waveguide to infinity. That is, we require $u(x,y) \to 0$ as $|x| \to \infty$, $|y| < 1$. It is instructive to consider separation solutions for the strip in the absence of the cut. A superposition of these solutions could be used to construct general solutions in two domains $x > a$ and $x < -a$ although such an approach will not be taken here.

In the symmetric case, separation solutions are

$$\{\cos(p^s_n y)\mathrm{e}^{\pm \mathrm{i}k^s_n x}\} \qquad \text{and} \qquad \{\cos(p^s_n y)\mathrm{e}^{\pm \kappa^s_n x}\}, \qquad \text{for } n \geq 1 \tag{9}$$

where $p^s_n = (n-\frac{1}{2})\pi$ and $k^s_n = (k^2-(p^s_n)^2)^{1/2} = -\mathrm{i}((p^s_n)^2-k^2)^{1/2}$ whilst $\kappa^s_n = (k^2+(p^s_n)^2)^{1/2}$. Thus, propagating modes only exist provided $k > \frac{1}{2}\pi$. The frequency ω^s_c defined by the relationship $k = \frac{1}{2}\pi$ (i.e. $\omega^s_c = (\frac{1}{16}D\pi^4/\rho h)^{1/2}$) is called the *first cut-off* frequency for symmetric modes, and thus $k < \frac{1}{2}\pi$ implies $\omega < \omega_c$, or that the frequency is below the first cut-off frequency.

In the antisymmetric case, separation solutions for u^a are given by

$$\{\sin(p^a_n y)\mathrm{e}^{\pm \mathrm{i}k^a_n x}\} \qquad \text{and} \qquad \{\sin(p^a_n y)\mathrm{e}^{\pm \kappa^a_n x}\}, \qquad \text{for } n \geq 1 \tag{10}$$

where $p_n^a = n\pi$ and $k_n = (k^2 - (p_n^a)^2)^{1/2} = -\mathrm{i}((p_n^a)^2 - k^2)^{1/2}$ whilst $\kappa_n^a = (k^2 + (p_n^a)^2)^{1/2}$. Now the first cut-off frequency ω_c^a is defined by the relationship $k = \pi$ and for frequencies below the cut-off (i.e. for $k < \pi$), no bounded waves are able to propagate to infinity along the strip.

The existence of cut-off frequencies below which no propagating waves exist for a uniform waveguide implies the possibility of trapping modes for frequencies $\omega < \omega_c^{s/a}$ represented by local vibrations in the presence of the cut in the strip.

3. Scattering by semi-infinite cuts and the wide-spacing approximation

In this section we consider scattering problems involving a cut of semi-infinite extent along the centreline $y = 0$ of the simply-supported wave guide. Hence, in this section, $\mathcal{C} = \{x : x > 0\}$. Specifically waves incident from $x = +\infty$ on the end of the cut at $x = 0$ are considered.

Symmetric solutions are generated by waves incident in $y > 0$ and $y < 0$ each side of the cut which are in phase. This ensures a symmetric response so that the total displacement satisfies (4). Thus solutions u^s of (1) may be sought in the domain $0 < y < 1$ when supplemented by (6)(b) and (3); the extension of the solution into $-1 < y < 0$ is provided by (4).

Likewise, antisymmetric solutions are generated by incident waves above and below the cut which are exactly out of phase with one another. Again we need only seek solutions u^a to (1) in the domain $0 < y < 1$ once the conditions (6)(a) and (3) have been applied; now the extension of the solution into $-1 < y < 0$ is provided by (5).

We need to consider the form of the wave incident in $0 < y < 1$, $x \in \mathcal{C}$ from $x = \infty$. First, in the symmetric case, solutions of the form $\mathrm{e}^{\pm\mathrm{i}\alpha x} F^s(\alpha, y)$ satisfying (1), (2) and (3)(b) we find

$$F^s(\alpha, y) = \frac{1}{2k^2}\left(\frac{L(\alpha)\sinh\lambda(1-y)}{\lambda\cosh\lambda} - \frac{G(\alpha)\sinh\gamma(1-y)}{\gamma\cosh\gamma}\right) \qquad (11)$$

in which

$$\lambda = \sqrt{\alpha^2 - k^2} = -\mathrm{i}\sqrt{k^2 - \alpha^2}, \qquad \gamma = \sqrt{\alpha^2 + k^2} \qquad (12)$$

and

$$L(\alpha) = (1-\nu)\alpha^2 - k^2, \qquad G(\alpha) = (1-\nu)\alpha^2 + k^2. \qquad (13)$$

Some of the notation is recycled from Norris & Wang [11]. In the antisymmetric case we seek solutions of the same form $\mathrm{e}^{\pm \mathrm{i}\alpha x}F^a(\alpha, y)$ satisfying (1), (2) and (3)(a) which result in

$$F^a(\alpha, y) = \frac{1}{2k^2}\left(\frac{G(\alpha)\sinh\lambda(1-y)}{\sinh\lambda} - \frac{L(\alpha)\sinh\gamma(1-y)}{\sinh\gamma}\right). \tag{14}$$

If we now apply (3)(a) to (11) and (3)(b) to (14) we obtain the same dispersion relation governing the propagating waves in $x > 0$, namely

$$E^s(\alpha) \equiv -\frac{\tanh\lambda\tanh\gamma}{\lambda\gamma}E^a(\alpha) \equiv \frac{L^2(\alpha)\tanh\lambda}{\lambda} - \frac{G^2(\alpha)\tanh\gamma}{\gamma} = 0 \tag{15}$$

(the definition of $E^{s/a}$ is for later use). It is straightforward to confirm that there are no real roots of (15) when $|\alpha| > k$ for values of ν in the physical range $-1 < \nu < \frac{1}{2}$. For $|\alpha| < k$, there exists a finite number of solutions of (15) depending on the value of k. For k below the first positive solution of

$$\tan k = \tanh k \tag{16}$$

(approximately $k \lesssim \frac{5}{4}\pi$) there are just a single pair of roots of (15) at $\alpha = \pm\alpha_0$, say. Extra pairs of roots of (15) are cut-on as k increases through the sequence of values defined by (16). Since previous arguments have already restricted our focus on $k < \frac{1}{2}\pi$ and $k < \pi$ in the symmetric and antisymmetric cases so it follows that we will only have need to consider this single pair of roots $\pm\alpha_0$.

It follows that the incident wave in $x > 0$, $0 < y < 1$ can be written as either

$$u^{s/a}_{inc}(x, y) = \mathrm{e}^{-\mathrm{i}\alpha_0 x}F^{s/a}(\alpha_0, y) \tag{17}$$

which only differ by a constant factor of $G(\alpha_0)\lambda\coth\lambda/L(\alpha_0)$. As indicated by the notation, these two different forms will be used in the appropriate symmetric and antisymmetric scattering problems.

The radiation conditions to apply in $0 < y < 1$ are: (i) that $u^{s/a} \to 0$ as $x \to -\infty$; and (ii)

$$u^{s/a}(x, y) \sim (\mathrm{e}^{-\mathrm{i}\alpha_0 x} + R^{s/a}\mathrm{e}^{\mathrm{i}\alpha_0 x})F^{s/a}(\alpha_0, y), \qquad \text{as } x \to \infty. \tag{18}$$

where $R^{s/a}$ are reflection coefficients to be found. Since there is total reflection and this is a system with no dissipation we anticipate that $|R^{s/a}| = 1$ (indeed this will be confirmed) and thus it is the phase of $R^{s/a}$ that we seek.

3.1. Solution of a scattering problem by the Wiener-Hopf method

We consider first the symmetric problem and define the Fourier transform

$$U^s(\alpha, y) = \int_{-\infty}^{\infty} (u^s(x, y) - u^s_{inc}(x, y))\mathrm{e}^{\mathrm{i}\alpha x} dx \tag{19}$$

so that from (1)

$$\left(\frac{d^2}{dy^2} - \lambda^2\right)\left(\frac{d^2}{dy^2} - \gamma^2\right) U^s(\alpha, y) = 0 \tag{20}$$

where λ, γ are defined by (12). We assume that k has a small imaginary part characterised by a parameter ϵ such that the imaginary part of α_0 is greater than ϵ which ensures that $U^s(\alpha, y)$ is analytic in the strip $\mathcal{D} = \{|\Im\{\alpha\}| < \epsilon\}$; eventually we shall let $\epsilon \to 0$. Then we have

$$U^s(\alpha, y) = U^s_+(\alpha, y) + U^s_-(\alpha, y) \tag{21}$$

where

$$\left.\begin{aligned} U^s_+(\alpha, y) &= \int_0^{\infty} (u^s(x, y) - u^s_{inc}(x, y))\mathrm{e}^{\mathrm{i}\alpha x}\,\mathrm{d}x, \\ U^s_-(\alpha, y) &= \int_{-\infty}^{0} (u^s(x, y) - u^s_{inc}(x, y))\mathrm{e}^{\mathrm{i}\alpha x}\,\mathrm{d}x \end{aligned}\right\} \tag{22}$$

and it follows that $U^s_{\pm}(\alpha, y)$ is analytic in $\mathcal{D}^{\pm}$ where $\mathcal{D}^+ = \{\Im(\alpha) > -\epsilon\}$, $\mathcal{D}^- = \{\Im(\alpha) < \epsilon\}$ and so $\mathcal{D} = \mathcal{D}^+ \cap \mathcal{D}^-$.

From (2) we require

$$U^s(\alpha, 1) = U^{s''}(\alpha, 1) = 0 \tag{23}$$

(primes denoting differentiation with respect to y) whilst from (7)(b),

$$(\overline{\mathcal{S}}U^s)(\alpha) \equiv U^{s'''}(\alpha, 0) - (2 - \nu)\alpha^2 U^{s'}(\alpha, 0) = 0. \tag{24}$$

A solution of (20) satisfying (23) and (24) is clearly

$$U^s(\alpha, y) = A^s(\alpha)F^s(\alpha, y) \tag{25}$$

where $F^s(\alpha, y)$ is given by (11). Now from (6)(b)

$$U^{s'}(\alpha, 0) = U^{s'}_+(\alpha, 0) - \int_{-\infty}^{0} \partial_y(u^s_{inc}(x, 0))\mathrm{e}^{\mathrm{i}\alpha x}\,\mathrm{d}x \tag{26}$$

or, from (17) and (25) and noting that $F^{s'}(\alpha,0)=1$,

$$U^{s'}(\alpha,0)=A^s(\alpha)=U_+^{s'}(\alpha,0)+\mathrm{i}/(\alpha-\alpha_0). \tag{27}$$

Finally from (3)(a) we have,

$$(\overline{\mathcal{B}}U^s)(\alpha)=(\overline{\mathcal{B}}U_-^s)(\alpha)=A^s(\alpha)(\overline{\mathcal{B}}F^s)(\alpha)=A^s(\alpha)E^s(\alpha)/(2k^2) \tag{28}$$

where $(\overline{\mathcal{B}}U)(\alpha)\equiv U''(\alpha,0)-\nu\alpha^2U(\alpha,0)$ and $E^s(\alpha)$ is defined in (15). Elimination of $A^s(\alpha)$ between (27) and (28) gives

$$K^s(\alpha)(\overline{\mathcal{B}}U_-^s)(\alpha)=U_+^{s'}(\alpha)+\mathrm{i}/(\alpha-\alpha_0) \tag{29}$$

where now

$$K^s(\alpha)\equiv\frac{2k^2}{E^s(\alpha)}. \tag{30}$$

It is shown in the Appendix that we may write $K^s(\alpha)=K_+^s(\alpha)K_-^s(\alpha)$ where $K_\pm^s(\alpha)$ is non-zero and analytic in $\mathcal{D}^\pm$. This allows us to rearrange (29) in the form

$$K_-^s(\alpha)(\overline{\mathcal{B}}U_-^s)(\alpha)-\frac{\mathrm{i}}{(\alpha-\alpha_0)K_+^s(\alpha_0)}=\frac{U_+^{s'}(\alpha)}{K_+^s(\alpha)}+\frac{\mathrm{i}}{(\alpha-\alpha_0)}\left(\frac{1}{K_+^s(\alpha)}-\frac{1}{K_+^s(\alpha_0)}\right) \tag{31}$$

where the left and right hand sides of (31) are now analytic in $\mathcal{D}^+$ and $\mathcal{D}^-$ respectively. The usual Wiener-Hopf arguments now apply. Thus, it is shown in the Appendix (see (A.8) that $K_\pm^s(\alpha)=O(|\alpha|^{-1/2})$ as $|\alpha|\to\infty$ whilst the edge behaviour (8) allows us to infer from the definitions of Fourier transforms (see later equations (57) and (65)) that $U^s(\alpha,y)=O(|\alpha|^{-5/2})$, $U^{s'}(\alpha,y)=O(|\alpha|^{-3/2})$ and $(\overline{\mathcal{B}}U^s)(\alpha)=O(|\alpha|^{-1/2})$ as $|\alpha|\to\infty$. This allow us to assert that both sides of (31) must vanish like $O(\alpha^{-1})$ as $|\alpha|\to\infty$ within the strip $\mathcal{D}$ and, by Liouville's theorem, it follows that both sides equate to zero.

Thus, for example,

$$(\overline{\mathcal{B}}U_-^s)(\alpha)=\frac{\mathrm{i}}{(\alpha-\alpha_0)K_+^s(\alpha_0)K_-^s(\alpha)} \tag{32}$$

which, when combined with (28), gives

$$A^s(\alpha)=\frac{2\mathrm{i}k^2}{(\alpha-\alpha_0)K_+^s(\alpha_0)K_-^s(\alpha)E^s(\alpha)} \tag{33}$$

or, from (30)

$$A^s(\alpha) = \frac{\mathrm{i}K^s_+(\alpha)}{(\alpha-\alpha_0)K^s_+(\alpha_0)}. \tag{34}$$

It follows from (19) that we can write either

$$u^s(x,y) - u^s_{inc}(x,y) = \frac{\mathrm{i}}{2\pi}\int_{-\infty}^{\infty} \frac{2k^2F^s(\alpha,y)\mathrm{e}^{-\mathrm{i}\alpha x}}{(\alpha-\alpha_0)K^s_+(\alpha_0)K^s_-(\alpha)E^s(\alpha)}\,d\alpha \tag{35}$$

or

$$u^s(x,y) - u^s_{inc}(x,y) = \frac{\mathrm{i}}{2\pi}\int_{-\infty}^{\infty} \frac{K^s_+(\alpha)F^s(\alpha,y)\mathrm{e}^{-\mathrm{i}\alpha x}}{(\alpha-\alpha_0)K^s_+(\alpha_0)}\,d\alpha. \tag{36}$$

This latter version is suitable for $x < 0$ since we see there is a single pole at $\alpha = \alpha_0$ which, after deforming the contour upwards, contributes the term $-F^s(\alpha_0, y)\mathrm{e}^{-\mathrm{i}\alpha_0 x}$. As expected, this eliminates the incident wave from the left-hand side of (36) and this ensures that $u^s(x,y) \to 0$ as $x \to -\infty$. We note that we have assumed $k < \pi/2$ which ensured there are no real poles of $F^s(\alpha, y)$ contributing to the far field.

To determine the phase of the reflected wave we deform downwards the contour of integration in (35). In the course of deformation we pick up a contribution from the pole at $\alpha = -\alpha_0$ due to the zero of $E^s(\alpha)$ at this point. Note again that there are no other real poles since $k < \frac{1}{2}\pi$. Thus we obtain

$$u^s(x,y) - u^s_{inc}(x,y) \sim -\frac{k^2F^s(-\alpha_0,y)\mathrm{e}^{\mathrm{i}\alpha_0 x}}{\alpha_0 K^s_+(\alpha_0)K^s_-(-\alpha_0)E^{s'}(-\alpha_0)} \tag{37}$$

so that the reflection coefficient, from (18) is

$$R^s = -\frac{k^2}{\alpha_0 K^s_+(\alpha_0)K^s_-(-\alpha_0)E^{s'}(-\alpha_0)}. \tag{38}$$

The Appendix shows how Cauchy's integral method can be used to split the function $K^s(\alpha)$ into plus/minus functions and that, as a result, we can write

$$R^s = -\left(\frac{k+\mathrm{i}\alpha_0}{k-\mathrm{i}\alpha_0}\right)^{1/2}\mathrm{e}^{2\mathrm{i}I^s(\alpha_0)} \tag{39}$$

where $I^s(\alpha)$ is defined by (A.7). This demonstrates that $|R^s| = 1$, as expected. Writing $R^s = \mathrm{e}^{2\mathrm{i}\delta^s}$ gives

$$\delta^s = \tfrac{1}{2}\pi + \tfrac{1}{2}\tan^{-1}(\alpha_0/k) + I^s(\alpha_0). \tag{40}$$

3.2. The antisymmetric problem

The changes are minor and we follow the solution method from §3.1 with the functions u^a and U^a replacing u^s and U^s. Thus, $U^a(\alpha, y)$ satisfies (20) and (23) as before but now (24) is replaced by

$$(\overline{\mathcal{B}}U^a)(x) \equiv U^{a\prime\prime}(\alpha) - \nu\alpha^2 U^a(\alpha) = 0 \tag{41}$$

on account of u^a satisfying (7)(b). It follows that we may write

$$U^a(\alpha, y) = A^a(\alpha)F^a(\alpha, y) \tag{42}$$

where $F^a(\alpha, y)$ is given by (14). Since condition (6)(a) replaces (6)(b) we have, instead of (26),

$$U^a(\alpha, 0) = U^a_+(\alpha, 0) - \int_{-\infty}^{0} u^a_{inc}(x, 0)\mathrm{e}^{\mathrm{i}\alpha x}\,\mathrm{d}x \tag{43}$$

or, from (42) and noting that $F^a(\alpha, 0) = 1$,

$$U^a(\alpha, 0) = A^a(\alpha) = U^a_+(\alpha, 0) + \mathrm{i}/(\alpha - \alpha_0). \tag{44}$$

Finally from (3)(b) we have,

$$(\overline{\mathcal{S}}U^a)(\alpha) = (\overline{\mathcal{S}}U^a_-)(\alpha) = A^a(\alpha)(\overline{\mathcal{S}}F^a)(\alpha) = A(\alpha)E^a(\alpha)/(2k^2) \tag{45}$$

where $\overline{\mathcal{S}}$ and $E^a(\alpha)$ are defined in (24) and (15) respectively. Elimination of $A^a(\alpha)$ now gives

$$K^a(\alpha)(\overline{\mathcal{S}}U^s_-)(\alpha) = U^a_+(\alpha) + \mathrm{i}/(\alpha - \alpha_0) \tag{46}$$

where

$$K^a(\alpha) = \frac{2k^2}{E^a(\alpha)}. \tag{47}$$

The argument now proceeds exactly as in §3.1 with the calculation of the reflection coefficient leading to

$$R^a = -\frac{k^2}{\alpha_0 K^a_+(\alpha_0)K^a_-(-\alpha_0)E^{a\prime}(-\alpha_0)}. \tag{48}$$

Equation (A.17) of the Appendix shows how this can be evaluated using the Cauchy integral formula and hence finally $R^a = \mathrm{e}^{2\mathrm{i}\delta^a}$ where

$$\delta^a = \tfrac{1}{2}\pi - \tfrac{1}{2}\tan^{-1}(\alpha_0/k) + I^a(\alpha_0). \tag{49}$$

with $I^a(\alpha)$ given by (A.15).

3.3. Wide-spacing approximation

We now consider the finite cut between $x = -a$ and $x = a$. Assuming that a is large enough so that only propagating waves interact between the two ends it is possible to choose the length of the crack so that phased-matched permanent reflections occur between the two ends of the crack. This wide-spacing argument is commonly-used to motivate and locate approximate trapped mode configurations; see for example Martin [12]).

Then we require

$$\frac{d}{dx}\left(\mathrm{e}^{-\mathrm{i}\alpha_0(x+a)} + R^{s/a}\mathrm{e}^{\mathrm{i}\alpha_0(x+a)}\right) = 0, \qquad \text{on } x = 0 \tag{50}$$

to approximate trapped modes which are symmetric about $x = 0$ and

$$\mathrm{e}^{-\mathrm{i}\alpha_0(x+a)} - R^{s/a}\mathrm{e}^{\mathrm{i}\alpha_0(x+a)} = 0, \qquad \text{on } x = 0 \tag{51}$$

for trapped modes antisymmetric about $x = 0$. With $R^{s/a} = \mathrm{e}^{2\mathrm{i}\delta^{s/a}}$ with $\delta^{s/a}$ given by (40), (49) these two combine to give the relation

$$a = (\tfrac{1}{2}n\pi - \delta^{s/a})/\alpha_0 \tag{52}$$

where n is odd(even) for trapped modes which are antisymmetric(symmetric) about $x = 0$.

4. Integral equation methods for the finite length cut

Consider first the symmetric problem for $u(x, y) \equiv u^s(x, y)$ satisfying (1)–(3) and (6)(b) with $\mathcal{C} = \{x : |x| < a\}$. We adopt the Fourier transform approach developed in §3.1 for scattering of incident waves with one minor change: here we remove the incident wave $u^s_{inc}(x, y)$ from the definition (19) as it is now being applied to a trapped mode problem. We follow the development in §3.1 which uses transformed versions of (1), (2) and (7)(b) (which subsumes (3)(b)) and leads to (25):

$$U^s(\alpha, y) = A^s(\alpha)F^s(\alpha, y). \tag{53}$$

Now, using (4)(b) we have

$$U^{s'}(\alpha, 0) = \int_{-a}^{a} u^s_y(x, 0)\mathrm{e}^{\mathrm{i}\alpha x}\,\mathrm{d}x \tag{54}$$

and, since $F^{s'}(\alpha,0)=1$, it follows that $A^s(\alpha)=U^{s'}(\alpha,0)$. Using this in (53), taking inverse transforms and reinvoking the definition of $U^{s'}(\alpha,0)$ in terms of $u^s_y(x,0)$ along $|x|<a$ from (54), shows that the solution may be written

$$u^s(x,y)=\frac{1}{2\pi}\int_{-\infty}^{\infty}\mathrm{e}^{-\mathrm{i}\alpha x}F^s(\alpha,y)\int_{-a}^{a}u^s_y(x',0)\mathrm{e}^{\mathrm{i}\alpha x'}\,\mathrm{d}x'\,\mathrm{d}\alpha \tag{55}$$

in terms of the unknown function $u^s_y(x,0)$ on the cut. This is determined by applying the remaining condition (3)(a) namely $(\mathcal{B}u^s)(x)=0$ on $y=0$ between $-a<x<a$. This results in

$$0=\frac{1}{4\pi k^2}\int_{-\infty}^{\infty}\mathrm{e}^{-\mathrm{i}\alpha x}E^s(\alpha)\int_{-a}^{a}u^s_y(x',0)\mathrm{e}^{\mathrm{i}\alpha x'}\,\mathrm{d}x'\,\mathrm{d}\alpha \tag{56}$$

for $|x|<a$ where $E^s(\alpha)$ is defined by (15). We note that

$$\int_{-a}^{a}u^s_y(x,0)\mathrm{e}^{\mathrm{i}\alpha x}\,\mathrm{d}x\sim O(|\alpha|^{-3/2}) \tag{57}$$

as $|\alpha|\to\infty$ which is readily derived as a consequence of the end-point behaviour of $u^s_y(x,0)$ expressed in (8).

The behaviour of $E^s(\alpha)$ for large $|\alpha|$ is described by (A.3) and can be used to write (56) as

$$\begin{aligned}0 &= \frac{1}{4\pi k^2}\int_{-\infty}^{\infty}\mathrm{e}^{-\mathrm{i}\alpha x}\left[E^s(\alpha)+4k^2|\alpha|\sigma\right]\int_{-a}^{a}u^s_y(x',0)\mathrm{e}^{\mathrm{i}\alpha x'}\,\mathrm{d}x'\,\mathrm{d}\alpha\\ &\quad -\frac{\sigma}{\pi}\int_{-\infty}^{\infty}|\alpha|\mathrm{e}^{\mathrm{i}\alpha x}\int_{-a}^{a}u_y(x',0)\mathrm{e}^{\mathrm{i}\alpha x'}\,\mathrm{d}x'\,\mathrm{d}\alpha.\end{aligned} \tag{58}$$

Now it can be shown from the following definition of the logarithm (Gradshteyn & Ryzhik [7, eqn.3.943]).

$$\log|x|=\frac{1}{2}\int_{-\infty}^{\infty}\frac{\mathrm{e}^{-|l|}-\mathrm{e}^{\mathrm{i}lx}}{|l|}\,\mathrm{d}l \tag{59}$$

that we can write (58) as

$$\begin{aligned}0 &= \frac{2\sigma}{\pi}\frac{d^2}{dx^2}\int_{-a}^{a}u_y(x',0)\log|x-x'|dx'\\ &\quad +\frac{1}{4\pi k^2}\int_{-\infty}^{\infty}\mathrm{e}^{-\mathrm{i}\alpha x}\left[E^s(\alpha)+4k^2|\alpha|\sigma\right]\int_{-a}^{a}u_y(x',0)\mathrm{e}^{\mathrm{i}\alpha x'}\,dx'\,d\alpha\end{aligned} \tag{60}$$

for $|x|<a$. The term in square brackets is $O(|\alpha|^{-3})$ as $|\alpha|\to\infty$.

4.1. The antisymmetric case

The approach is the same as in the previous section and the changes needed are minor. We follow the Fourier transform approach for $u^a(x,y)$ which leads to (42):

$$U^a(\alpha,y) = A^a(\alpha)F^a(\alpha,y). \tag{61}$$

On account of (6)(a) we have

$$U^a(\alpha,0) = \int_{-a}^{a} u^a(x,0)\mathrm{e}^{\mathrm{i}\alpha x}\,\mathrm{d}x \tag{62}$$

and since $F^a(\alpha,0)=1$ it follows that $A^a(\alpha)=U^a(\alpha,0)$.

The inverse transform gives

$$u^a(x,y) = \frac{1}{2\pi}\int_{-\infty}^{\infty}\mathrm{e}^{-\mathrm{i}\alpha x}F^a(\alpha,y)\int_{-a}^{a}u^a(x',0)\mathrm{e}^{\mathrm{i}\alpha x'}\,\mathrm{d}x'\,\mathrm{d}\alpha \tag{63}$$

in terms of the unknown displacement along the cut from $-a<x<a$. This representation automatically satisfies $(\mathcal{B}u^a)(x)=0$ and thus we only require to apply the condition $(\mathcal{S}u^a)(x)=0$ on $|x|<a$. This gives

$$0 = \frac{1}{4\pi k^2}\int_{-\infty}^{\infty}\mathrm{e}^{-\mathrm{i}\alpha x}E^a(\alpha)\int_{-a}^{a}u^a(x',0)\mathrm{e}^{\mathrm{i}\alpha x'}\,\mathrm{d}x'\,\mathrm{d}\alpha, \qquad |x|<a \tag{64}$$

where $E^a(\alpha)$ is given by (15). Here, we can show that

$$\int_{-a}^{a}u^a(x,0)\mathrm{e}^{\mathrm{i}\alpha x}\,\mathrm{d}x \sim O(|\alpha|^{-5/2}) \tag{65}$$

as $|\alpha|\to\infty$ whilst the behaviour for large α of $E^a(\alpha)$ is given after (A.12). Using the mechanism of the previous section, in which the leading order behaviour of $E^a(\alpha)$ is subtracted and added back on, with the use of (59) we may write (64) as

$$\begin{aligned} 0 \;=\; & -\frac{2\sigma}{\pi}\frac{d^4}{dx^4}\int_{-a}^{a}u^a(x',0)\log|x-x'|\mathrm{d}x' \\ & +\frac{1}{4\pi k^2}\int_{-\infty}^{\infty}\mathrm{e}^{-\mathrm{i}\alpha x}\left[E^a(\alpha)+4k^2|\alpha|^3\sigma\right]\int_{-a}^{a}u^a(x',0)\mathrm{e}^{\mathrm{i}\alpha x'}\,\mathrm{d}x'\,\mathrm{d}\alpha \end{aligned} \tag{66}$$

for $|x|<a$. The term in square brackets is $O(|\alpha|^{-1})$ as $|\alpha|\to\infty$.

4.2. Approximation of solutions to integral equations

In this section we describe how the Galerkin method can be used to solve the integro-differential equations (60) and (66) above.

Taking into account the behaviour (4), we make the following expansions for the two unknown functions in the symmetric and antisymmetric problems:

$$u^s_y(x,0) = \sum_{n=0}^{\infty} \alpha^s_n p_n(x), \qquad \text{and} \qquad u^a(x,0) = \sum_{n=0}^{\infty} \alpha^a_n q_n(x), \qquad |x| < a, \tag{67}$$

where

$$p_n(x) = \frac{\mathrm{e}^{-\mathrm{i}n\pi/2}}{(n+1)a}(a^2 - x^2)^{1/2} U_n(x/a), \tag{68}$$

and

$$q_n(x) = \frac{2\mathrm{e}^{-\mathrm{i}n\pi/2}}{(n+1)(n+2)(n+3)a^2}(a^2 - x^2)^{3/2} C^{(2)}_n(x/a). \tag{69}$$

In the above U_n and $C^{(2)}_n$ are orthogonal second-kind Chebychev and Gegenbauer polynomials (respectively). The particular choice of orthogonal polynomials are made because of their association with the weighting functions in (68) and (69). In particular, they satisfy the orthogonality relationships

$$\int_{-a}^{a} (a^2 - x^2)^{1/2} U_n(x/a) U_m(x/a) dx = \tfrac{1}{2}\pi a^2 \delta_{mn}; \tag{70}$$

and

$$\int_{-a}^{a} (a^2 - x^2)^{3/2} C^{(2)}_n(x/a) C^{(2)}_m(x/a) dx = \tfrac{1}{8}\pi a^4 (m+3)(m+1)\delta_{mn}. \tag{71}$$

(Gradshteyn & Ryzhik [7, eqn. 7.313]) Various relationships involving these functions hold which will be useful. First we have

$$\frac{d^2}{dx^2} \int_{-a}^{a} \ln|x - x'| (a^2 - x'^2)^{1/2} U_n(x'/a) dx' = \pi(n+1) U_n(x/a) \tag{72}$$

and

$$-\frac{d^4}{dx^4} \int_{-a}^{a} \ln|x - x'| (a^2 - x^2)^{3/2} C^{(2)}_n(x'/a) dx' = \pi(n+3)(n+2)(n+1) C^{(2)}_n(x/a) \tag{73}$$

(Andronov & Belinskii [1]) which demonstrate that the respective orthogonal polynomials are a natural choice, being eigenfunctions of the most singular part of the integral operator in each of the two cases.

Also needed in making the required calculations that follow are the results

$$\int_{-a}^{a} \mathrm{e}^{\mathrm{i}\alpha x}(a^2-x^2)^{1/2}U_n(x/a)dx = \frac{\mathrm{e}^{\mathrm{i}n\pi/2}(n+1)\pi a^2}{\alpha a}J_{n+1}(\alpha a) \tag{74}$$

and

$$\int_{-a}^{a} \mathrm{e}^{\mathrm{i}\alpha x}(a^2-x^2)^{3/2}C_n^{(2)}(x/a)dx = \frac{\mathrm{e}^{\mathrm{i}n\pi/2}(n+3)(n+2)(n+1)\pi a^4}{2(\alpha a)^2}J_{n+2}(\alpha a) \tag{75}$$

(Gradshteyn & Ryzhik [7, eqn.7.321]). We note in passing that the large $|\alpha|$ behaviour anticipated by (57) and (65) is exhibited in (74) and (75) once the large argument behaviour of Bessel functions has been used.

The Galerkin procedure involves substituting (69) into (60) or (66) and then multiplying through by $p_m^*(x)$ or $q_m^*(x)$ ($*$ denotes complex conjugate) for $m = 0, 1, 2, \ldots$ and integrating over $-a < x < a$. This results in the infinite system of equations for the unknown coefficients $\alpha_n^{s/a}$:

$$\frac{\alpha_m^s}{(m+1)} - \sum_{n=0}^{\infty} \alpha_n^s K_{mn}^s = 0, \qquad m = 0, 1, 2, \ldots \tag{76}$$

where

$$K_{mn}^s = \frac{1}{4k^2\sigma}\int_{-\infty}^{\infty} \left[4\sigma k^2|\alpha| + E^s(\alpha)\right] \frac{J_{n+1}(\alpha a)J_{m+1}(\alpha a)}{\alpha^2}\,\mathrm{d}\alpha; \tag{77}$$

and in the antisymmetric case

$$\frac{\alpha_m^a}{(m+2)} - \sum_{n=0}^{\infty} \alpha_n^a K_{mn}^a = 0, \qquad m = 0, 1, 2, \ldots \tag{78}$$

where

$$K_{mn}^a = \frac{1}{4k^2\sigma}\int_{-\infty}^{\infty} \left[4\sigma k^2\alpha^2|\alpha| + E^a(\alpha)\right] \frac{J_{n+2}(\alpha a)J_{m+2}(\alpha a)}{\alpha^4}\,\mathrm{d}\alpha. \tag{79}$$

In both (77) and (79) the integrands decay like $O(|\alpha|^{-6})$. Also, the symmetry of the terms contained in square brackets in α and the relation $J_n(-x) =$

$(-1)^n J_n(x)$ implies that $K^{s/a}_{mn} = 0$ when $m+n$ is odd. This allows (76) and (78) to decouple into even and odd systems which reflect the fact that we could have decomposed the system from the outset into modes which are symmetric/antisymmetric in x about $x = 0$. Explicitly these are

$$\frac{\alpha^s_{2m+\nu}}{(2m+1+\nu)} - \sum_{n=0}^{\infty} \alpha^s_{2n+\nu} K^s_{2m+\nu,2n+\nu} = 0, \qquad m = 0, 1, 2, \ldots \tag{80}$$

for $\nu = 0, 1$ for symmetric/antisymmetric modes, where

$$K^s_{2m+\nu,2n+\nu} = 2\int_0^{\infty} \left[\frac{E^s(\alpha)}{4k^2\alpha^2\sigma} + \frac{1}{\alpha}\right] J_{2n+1+\nu}(\alpha a) J_{2m+1+\nu}(\alpha a)\, d\alpha; \tag{81}$$

and in the antisymmetric case:

$$\frac{\alpha^a_{2m+\nu}}{(2m+2+\nu)} - \sum_{n=0}^{\infty} \alpha^a_{2n+\nu} K^a_{2m+\nu,2n+\nu} = 0, \qquad m = 0, 1, 2, \ldots \tag{82}$$

again where $\nu = 0, 1$ represents symmetry/antisymmetry in $x = 0$ and where

$$K^a_{2m+\nu,2n+\nu} = 2\int_0^{\infty} \left[\frac{E^a(\alpha)}{4k^2\alpha^4\sigma} + \frac{1}{\alpha}\right] J_{2n+2+\nu}(\alpha a) J_{2m+2+\nu}(\alpha a)\, d\alpha. \tag{83}$$

The systems of equations (80) and (82) should be computed numerically by truncation.

4.3. One term approximations

Truncating the systems (80) and (82) to just one term is equivalent to applying a variational approximation the integral equations whereby the unknown functions are approximated by a single function which accommodate the end point behaviours in (8). It is supposed here, and later confirmed numerically in the results section, that such an approximation will be effective if the length of cut is small compared to the wavelength of waves along the crack when the local variations in properties of u along the crack are small and that these are dominated by the end-point behaviour. Such an argument leads to simple relations which implicitly define the relation between a and k. For example, for trapped modes which symmetry in both $x = 0$ and $y = 0$ the one-term approximation is, from (80), given by

$$2\int_0^{\infty} \left[\frac{E^s(\alpha)}{4k^2\alpha^2\sigma} + \frac{1}{\alpha}\right] J_1^2(\alpha a)\, d\alpha = 1. \tag{84}$$

It is envisaged that this 'small-spacing' approximation will complement the wide-spacing approximation developed in §3.

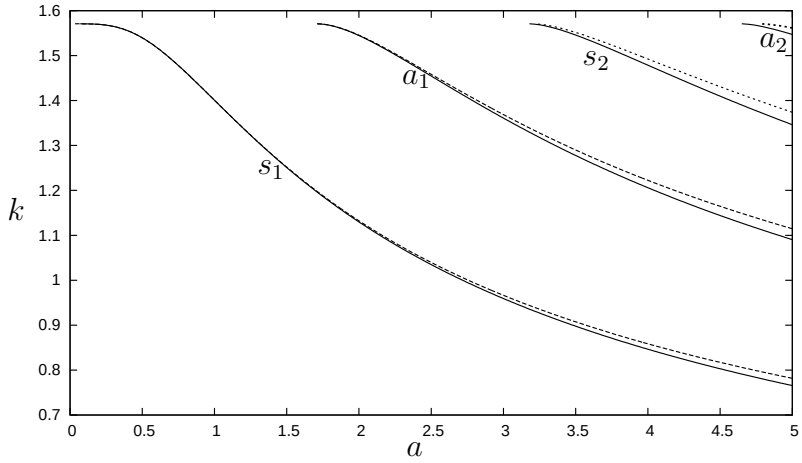

Figure 2: y-symmetric trapped mode relations (solid curves) computed using the integral equation method – s and a refer to symmetry and antisymmetry about $x = 0$. For s_1 and a_1 dashed line is the one-term approximation; for s_2 and a_2, dotted line is a two-term approximation.

5. Results

First, in figures 2 and 3 we show the trapped modes which are symmetric and antisymmetric in y computed using the integral equation method of §4. In all results shown we have chosen $\nu = 0.3$. In each plot, the solid curves represent converged solutions to the truncated numerical systems (80) and (82); these are relations between wavenumber k (and hence frequency) and cut length a. Within each set of results, more trapped modes are 'cut on' (through $k = \frac{1}{2}\pi$ or $k = \pi$ in the two different cases) as a increases and these alternate between modes which are symmetric and antisymmetric about the midpoint of the cut, $x = 0$. This feature is common for waveguide trapped modes (see Evans & Linton [4], for example) as more modes are able to occupy the increasing domain between the two ends of the crack.

Thus, we see that a mode symmetric in x exists for all a. Also shown on figures 2 and 3 using dashed/dotted lines are approximations to the trapped mode curves computed using either a one-term, two-term or three-term approximation to the infinite system of equations. We see that a one-term approximation is accurate for the first symmetric mode, especially as $a \to 0$, as we had expected. It also works well for the first antisymmetric mode. Increasing the approximation to two terms for a_1 and s_1 yields results which

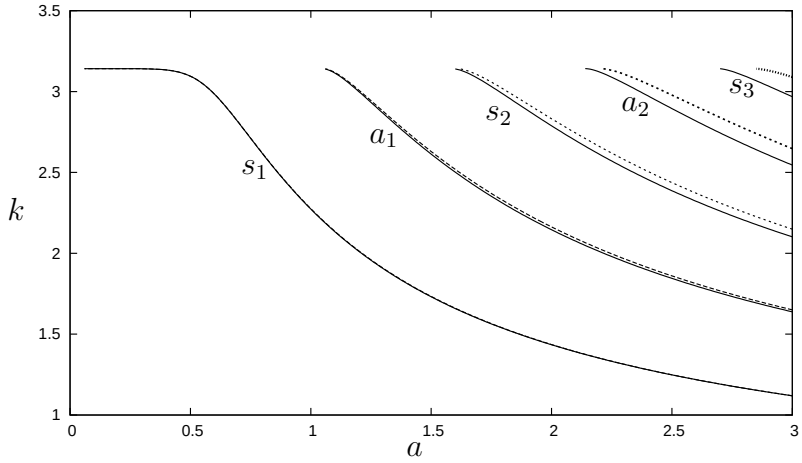

Figure 3: y-antisymmetric trapped mode relations (solid curves) computed using the integral equation method – s and a refer to symmetry and antisymmetry about $x = 0$. For s_1 and a_1 dashed line is the one-term approximation; for s_2 and a_2, dotted line is a two-term approximation; for s_3, dotted line is 3-term approximation.

are graphically indistinguishable from those for higher truncation sizes. This pattern is continued for higher order modes where an N term truncation is shown for modes labelled s_N and a_N and where, in general, an $N + 1$ term approximation is in very good agreement with higher truncation sizes. This increase in the truncation size with mode number is expected as the higher modes need to be adequately resolved by the polynomial approximation used in the Galerkin approach.

Next we compare, in figures 4, 5, the wide-spacing approximations (52) using reflected wave phases $\delta^{s/a}$ derived from the Wiener-Hopf analysis with the accurate converged numerical results from the integral equation method. The wide-spacing performs excellently even for small values of the spacing, a. This success is not unsurprising and is often observed in applications of the wide-spacing approximation.

6. Conclusions and discussion

In this paper, two approached have been described for estimating trapped mode frequencies for thin elastic plates held between parallel simple supports and containing a thin straight crack along the centreline. A Wiener-Hopf approach applied to the total reflection of waves travelling along the waveguide

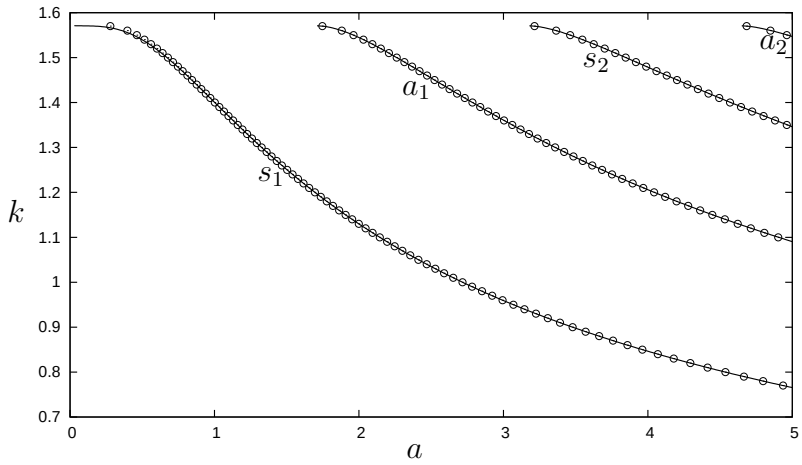

Figure 4: Comparison between wide-spacing approximation (circles) and converged integral equation results for y-symmetric trapped modes.

by the end of the crack is used to furnish an analytic expression for the phase of the reflection coefficient which is used in a wide-spacing approximation for the relationship between the wavenumber k of free waves in the plate (a proxy for the frequency) and a the half-length of the crack. A second approach seeks trapped modes directly through the formulation of integro-differential equations for unknown functions along the crack. By expanding these functions in an appropriate basis which takes into account properties of the plate displacement at the ends of the crack a Galerkin method converts the integro-differential equations into an infinite linear system of algebraic equations which are both simple to compute and converge rapidly with increasing truncation size. Indeed, it is shown how a novel explicit 'small-spacing' approximation associated with truncation to a 1×1 system of equations, gives accurate results for small values of a and thus complements the wide-spacing approximation. Indeed, the range of values of a over which the small-spacing and wide-spacing results remain accurate appear to overlap.

Both approaches are based on Fourier transforms taken along the waveguide. In both cases, the numerically difficult task of computing complex roots of the complicated dispersion relations which arise from separation of variables is avoided (the Wiener-Hopf approach requires a single real root to a dispersion relation to be computed, but this is a straightforward numerical

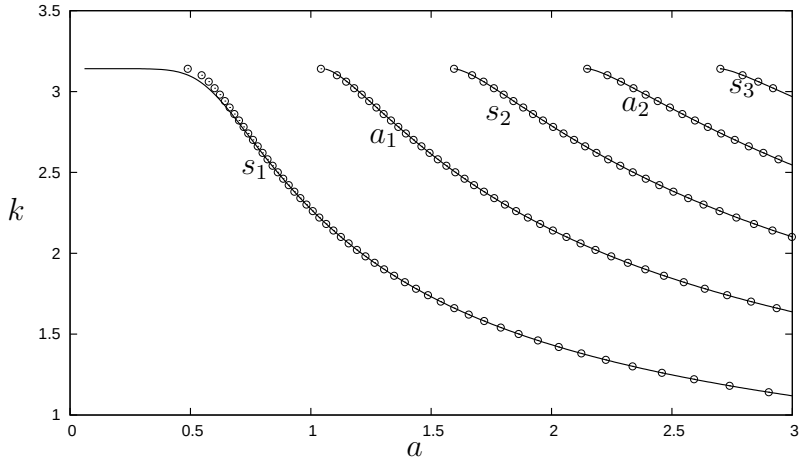

Figure 5: Comparison between wide-spacing approximation (circles) and converged integral equation results for y-symmetric trapped modes.

task). Thus, the simply-supported edges of the elastic plate – chosen to make the analysis digestible – could, for instance, be replaced by clamped or free edges. Whilst there would be an additional algebraic complication, particularly in analysing the dispersion relations that arise, there is no conceptual difficulty in applying the Wiener-Hopf or integral equation methods.

The formulation of integro-differential equations through the application of Fourier transforms to problems in which geometric boundaries of the domain are aligned seems natural. However, the authors are not aware of its widespread use in linear wave problems. Thus, it is more typical that Green's functions or eigenfunction matching approaches (which include modified residue calculus methods, e.g. Evans [5]) are employed. In light of the transform-based approach developed here, such approaches seem cumbersome, either requiring complicated analysis of hypersingular integral equations (e.g. Parsons & Martin [13], Martin [12]) or computation of complex roots of dispersion relations. Obvious extensions of the integral-equation formulation here are to plates in acoustic waveguides (e.g. Evans [5]), horizontal plates submerged below the free surface of a fluid (e.g. Evans & Peter [6], Evans & Linton [4]) and scattering by thin vertical offshore breakwaters (e.g. Linton & McIver [8]). In any such application it is envisaged that one-term small-spacing approximations similar to that described here will provide accurate results for small enough plate lengths.

Finally, given the evidence presented both here and in Porter [14] it is natural to seek a proof of the existence of trapped modes in the presence of an arbitrary-shaped hole with free edges (symmetric about the centreline) in a simply-supported waveguide. This could be done by adapting the proof of Evans et al. [3] for acoustic trapped modes. Following their approach, it is possible to adapt the variational principle of Porter & Porter [15] to show that the Rayleigh quotient for this problem is

$$R(u) = \frac{\iint_D \{(\nabla^2 u)^2 - 2(1-\nu)(u_{xx}u_{yy} - u_{xy}^2)\}\,\mathrm{d}x\mathrm{d}y}{\iint_D u^2\,\mathrm{d}x\mathrm{d}y}$$

where D is the domain occupied by the elastic plate excluding the hole. The natural conditions satisfied by u in the Rayleigh Quotient include the plate equation, the vanishing of the bending moment and shear stress on the free edge of the hole and $u_{yy} = 0$ on $y = \pm 1$. The essential condition on u is that $u = 0$ on $y = \pm 1$. By considering subspaces of functions which are symmetric/antisymmetric about $y = 0$ a proof would involve constructing trial functions, u, with continuous second derivatives which decay as $x \to \pm\infty$, are zero on $y = \pm 1$ and have the appropriate symmetries about $y = 0$ such that $R(u) < (\frac{1}{2}\pi)^4$ (or π^4) for the symmetric (antisymmetric) cases. A simple adaptation of the y-variation in the trial functions used by Evans et al. [3] fails to satisfy these inequalities.

Appendix A. Splitting of the functions $K^{s/a}(\alpha)$.

In the following we describe the Cauchy integral method for splitting the function $K^{s/a}(\alpha)$ into plus/minus functions. See also Norris & Wang [11] and Evans & Peter [6].

We start with $K^s(\alpha)$ and have from (25)

$$K^s(\alpha) = \frac{2k^2}{E^s(\alpha)} \tag{A.1}$$

where

$$E^s(\alpha) = L^2(\alpha)\frac{\tanh\gamma}{\gamma} - G^2(\alpha)\frac{\tanh\lambda}{\lambda} \tag{A.2}$$

Using the definitions of λ, γ and L and G it can be shown that

$$E^s(\alpha) \sim -4k^2\sigma|\alpha| + O(k^6/|\alpha|^3), \qquad \text{as } |\alpha| \to \infty \tag{A.3}$$

where $\sigma = \frac{1}{4}(1-\nu)(3+\nu)$. This implies that $K^s(\alpha) \sim -1/(2\sigma|\alpha|)$ as $|\alpha| \to \infty$. We write

$$M^s(\alpha) \equiv (-2\sigma)(\alpha^2 - \alpha_0^2)K^s(\alpha)/\gamma(\alpha). \tag{A.4}$$

Now $M^s(\alpha)$ has no real poles for $k < \frac{1}{2}\pi$ since those at $\alpha = \pm\alpha_0$ in K^s are cancelled. Also $M^s(\alpha) \to 1$ as $|\alpha| \to \infty$ so that $\log M^s(\alpha) \to 0$ as $|\alpha| \to \infty$. We write

$$\log M^s_{\pm}(\alpha) = \pm\frac{1}{2\pi\mathrm{i}} \int_{\mathcal{C}_\pm} \frac{\log M^s(t)}{t-\alpha}\,\mathrm{d}t \tag{A.5}$$

where $\mathcal{C}_+(\mathcal{C}_-)$ is a contour along $-\infty < \Re(t) < \infty$ lying within the strip $\mathcal{D}$ and passing below(above) the point $\alpha \in \mathcal{D}$. If α is real we can deform the contours onto the real axis provided we indent above(below) the point α. We find that

$$M^s_{\pm}(\alpha) = (M^s(\alpha))^{1/2}\mathrm{e}^{\mp\mathrm{i}I^s(\alpha)} \tag{A.6}$$

where

$$I^s(\alpha) = \frac{\mathrm{sgn}(\alpha)}{\pi}\int_0^\infty \frac{\log M^s(\alpha t)}{t^2-1}\,\mathrm{d}t = \frac{\mathrm{sgn}(\alpha)}{\pi}\int_0^1 \frac{\log[M^s(\alpha/t)/M^s(\alpha t)]}{1-t^2}\,\mathrm{d}t \tag{A.7}$$

after splitting the range of integration and writing $1/t$ for t, so that the principal-value integral is now well-behaved at $t = 1$. Also from its definition we have $M^s_+(\alpha) = M^s_-(-\alpha)$. It follows from (A.4) that K^s can be split into functions $K^s_\pm$ analytic in $\mathcal{D}^\pm$ given by

$$K^s_{\pm}(\alpha) = \frac{(k \mp \mathrm{i}\alpha)^{1/2}(M^s(\alpha))^{1/2}\mathrm{e}^{\mp\mathrm{i}I^s(\alpha)}}{(\alpha \pm \alpha_0)(-2\sigma)^{1/2}} \tag{A.8}$$

after splitting $\gamma(\alpha) = (k - \mathrm{i}\alpha)^{1/2}(k + \mathrm{i}\alpha)^{1/2}$. This implies that $K^s_+(\alpha) = -K^s_-(-\alpha)$ and so the product in the denominator of (38) is

$$\begin{aligned} K^s_+(\alpha)K^s_-(-\alpha) = -(K^s_+(\alpha))^2 &= \frac{(k-\mathrm{i}\alpha)M^s(\alpha)\mathrm{e}^{-2\mathrm{i}I^s(\alpha)}}{(2\sigma)(\alpha+\alpha_0)^2} \\ &= -2k^2\left(\frac{k-\mathrm{i}\alpha}{k+\mathrm{i}\alpha}\right)^{1/2}\left(\frac{\alpha-\alpha_0}{\alpha+\alpha_0}\right)\frac{\mathrm{e}^{-2\mathrm{i}I^s(\alpha)}}{E^s(\alpha)} \end{aligned} \tag{A.9}$$

after using (A.4) and (A.6). Finally we note that

$$\lim_{\alpha\to\alpha_0}\frac{(\alpha-\alpha_0)}{E^s(\alpha)} = \frac{1}{E^{s\prime}(\alpha_0)} \tag{A.10}$$

and that since E^s is even in α, $E^{s'}$ is odd in α implying from (38) that

$$R^s = -\frac{k^2}{\alpha_0 K_+^s(\alpha_0) K_-^s(-\alpha_0) E^{s'}(-\alpha_0)} = -\left(\frac{k+\mathrm{i}\alpha_0}{k-\mathrm{i}\alpha_0}\right)^{1/2} \mathrm{e}^{2\mathrm{i}I^s(\alpha_0)}. \quad \text{(A.11)}$$

The antisymmetric case follows in a similar manner. Thus we start with (47)

$$K^a(\alpha) = \frac{2k^2}{E^a(\alpha)} \quad \text{(A.12)}$$

and it can be shown that $E^a(\alpha) \sim 4k^2\sigma|\alpha|^3 + O(k^6/|\alpha|^3)$ as $|\alpha| \to \infty$, so that $K^a(\alpha) \sim 1/(2\sigma|\alpha|^3)$ as $|\alpha| \to \infty$. We write

$$M^a(\alpha) \equiv 2\sigma\gamma(\alpha)(\alpha^2 - \alpha_0^2)K^a(\alpha) \quad \text{(A.13)}$$

such that $M^a(\alpha)$ has no real poles for $k < \pi$, since those at $\alpha = \pm\alpha_0$ are cancelled. Also, $M^a(\alpha) \to 1$ so that $\log M^a(\alpha) \to 0$ as $|\alpha| \to \infty$. Proceeding as for $M^s(\alpha)$ above we obtain

$$K_\pm^a(\alpha) = \frac{(M^a(\alpha))^{1/2}\mathrm{e}^{\mp\mathrm{i}I^a(\alpha)}}{(k \mp \mathrm{i}\alpha)^{1/2}(2\sigma)^{1/2}(\alpha \pm \alpha_0)} \quad \text{(A.14)}$$

where

$$I^a(\alpha) = \frac{\mathrm{sgn}(\alpha)}{\pi}\int_0^1 \frac{\log[M^a(\alpha/t)/M^a(\alpha t)]}{1-t^2}\,\mathrm{d}t. \quad \text{(A.15)}$$

Again $K_+(\alpha) = -K_-(-\alpha)$, each decaying like $O(|\alpha|^{-3/2})$ as $|\alpha| \to \infty$, so that

$$\begin{aligned} K_+^a(\alpha)K_-^a(-\alpha) = -(K_+^a(\alpha))^2 &= \frac{M^a(\alpha)\mathrm{e}^{-2\mathrm{i}I^a(\alpha)}}{2\sigma(k-\mathrm{i}\alpha)(\alpha+\alpha_0)^2} \\ &= \left(\frac{k+\mathrm{i}\alpha}{k-\mathrm{i}\alpha}\right)^{1/2}\left(\frac{\alpha-\alpha_0}{\alpha+\alpha_0}\right)\frac{\mathrm{e}^{-2\mathrm{i}I^a(\alpha)}}{E^a(\alpha)}. \end{aligned} \quad \text{(A.16)}$$

As before $\lim_{\alpha\to\alpha_0}\{(\alpha-\alpha_0)/E^a(\alpha)\} = 1/E^{a'}(\alpha_0) = -1/E^{a'}(-\alpha_0)$ so that from (48)

$$R^a = -\frac{k^2}{\alpha_0 K_+^a(\alpha_0) K_-^a(-\alpha_0) E^{a'}(-\alpha_0)} = -\left(\frac{k-\mathrm{i}\alpha_0}{k+\mathrm{i}\alpha_0}\right)^{1/2} \mathrm{e}^{2\mathrm{i}I^a(\alpha_0)}. \quad \text{(A.17)}$$

References

[1] I.V. Andronov, B.P. Belinskii, Scattering of a flexural wave by a finite straight crack in an elastic plate, J. Sound Vib. 180(1)(1995) 1–16.

[2] M.A. Callan, C.M. Linton, D.V. Evans, Trapped modes in two-dimensional waveguides, J. Fluid Mech. 229 (1991) 51–64

[3] D.V. Evans, M. Levitan, D. Vassiliev Existence theorems for trapped modes, J. Fluid Mech. 261 (1994) 21–31.

[4] D.V. Evans, C.M. Linton Trapped modes in open channels, J. Fluid Mech. 225 (1991) 153–175.

[5] D.V. Evans, Trapped acoustic modes, J. Inst. Math. Appl. 49 (1992) 45–60.

[6] D.V. Evans, M.A. Peter, Asymptotic reflection of linear water waves by submerged horizontal porous plates, J. Eng. Math. 69(2-3) (2011) 135–154.

[7] I.S. Gradshteyn, I. M. Ryzhik, Table of Integrals, Series, and Products (4th Ed). Academic Press, New York (1980).

[8] C.M. Linton, P. McIver, Handbook of mathematical techniques for wave/structure interactions, CRC Press (2001).

[9] C.M. Linton, P. McIver, Embedded trapped modes in water waves and acoustics, Wave Motion 45(1-2) (2007) 16–29.

[10] C.M. Linton, D.V. Evans, Trapped modes above a submerged horizontal plate, Quart. J. Mech. Appl. Math. 44(3) (1991) 487–506.

[11] A.N. Norris, Z. Wang, Bending wave diffraction from strips and cracks on thin plates, Quart. J. Mech. Appl. Math. 47 (1994) 607–627.

[12] P.A. Martin, Multiple Scattering: Interaction of Time-Harmonic Waves with N obstacles. Cambridge University Press (2006).

[13] N.F. Parsons, P.A. Martin, Scattering of water waves by submerged plates using hypersingular integral equations, Appl. Ocean Res. 14 (1992) 313–321.

[14] R. Porter, Trapped modes in thin elastic plates, Wave Motion, 45(1-2) (2007), 3–15.

[15] D. Porter, R. Porter Approximations to wave scattering by an ice sheet of variable thickness over undulating topography, J. Fluid Mech. 509 (2004) 145–179.

[16] R. Porter, D.V. Evans Diffraction of flexural waves by finite straight cracks in an elastic sheet over water, J. Fluids Structures 23 (2007) 309–327.